N O T I C E

THIS DOCUMENT HAS BEEN REPRODUCED FROM MICROFICHE. ALTHOUGH IT IS RECOGNIZED THAT CERTAIN PORTIONS ARE ILLEGIBLE, IT IS BEING RELEASED IN THE INTEREST OF MAKING AVAILABLE AS MUCH INFORMATION AS POSSIBLE

AN INVESTIGATION OF THE CRATERING-INDUCED MOTIONS OCCURRING DURING THE FORMATION OF BOWL-SHAPED CRATERS

(NASA-CR-164186) AN INVESTIGATION OF THE CRATERING-INDUCED MOTIONS OCCURRING DURING THE FORMATION OF BOWL-SHAPED CRATERS Final Technical Report, 1 Jun. 1978 - 30 Jun. 1980 (Dayton Univ., Ohio.) 14 p HC A02/MF A01

N81-21989

Unclas
G3/91 42035

FINAL TECHNICAL REPORT

ANDREW J. PIEKUTOWSKI
PRINCIPAL INVESTIGATOR

June 1, 1978 to June 30, 1980

University of Dayton Research Institute
300 College Park Avenue
Dayton, Ohio 45469

Research Supported Under NASA Grant No. NSG-7444

INTRODUCTION

Studies of the impact craters formed on lunar and planetary surfaces have shown that bowl-shaped craters form the largest number and simplest class of craters observed on these surfaces. Several models which describe physical processes that may be associated with the formation of these craters have been proposed. However, none of these models provide quantitative data which describe the various dynamic processes that occur during the formation of this simplest class of crater.

Studies recently performed at the University of Dayton Research Institute under support provided by NASA Grant 7444 have permitted the effects of the dynamic processes which occur during crater formation to be examined in detail. In these studies, small hemispherical high-explosive charges were detonated in a tank which had one wall constructed of a thick piece of clear Plexiglas. Crater formation and the motions of numerous tracer particles installed in the cratering medium at the medium-wall interface were viewed through the wall of this quarter-space tank and recorded with high-speed cameras. Subsequent study and analysis of particle motions and events recorded on the film provide data needed to develop a time-sequence description of the formation of a bowl-shaped crater.

Although the crater formation process initiated by impact of a hypervelocity body is not identical with that initiated by detonation of a high-explosive, the processes are similar in terms of crater morphologies and structural deformations. Experimental uncertainties associated with impacting a cratering medium with a hypervelocity projectile at a precise location and time would result in a fairly low success rate for this type of experiment. Consequently, use of small high-explosive charges as the crater producing source simplifies experimental procedures and elevates the probability of success of each experiment.

EXPERIMENTAL PROGRAM

Twenty-three cratering experiments were performed. Eight of these experiments were performed in a normal half-space environment to provide benchmark crater dimension data. These data were used to supplement the large quantity of data available from experimental studies previously performed for the Air Force Weapons Laboratory. The remaining 15 experiments were performed in a quarter-space tank. Crater growth rate data were obtained from films of these experiments. In addition, variously colored sand grain tracers were installed at the cratering medium-tank wall interface for 11 of these experiments. Ten of these particle displacement experiments produced films which were analyzed to provide quantitative data that described the motions of the tracer grains and the behavior of material within regions bounded by sets of grains. Behavior of the material in these regions was inferred from the collective motions of each set of grains. Details of the various procedures used in the preparation of the experiments and reduction of data are provided in the attached paper entitled "Formation of Bowl-Shaped Craters".

Crater formation was examined in three media: (1) Ottawa Flint Shot, (2) Ottawa Banding Sand, and (3) desert alluvium. Two weights of pentaerythritol tetranitrate (PETN)- silver azide charges--0.40 g and 1.26 g-- and 1.70 g lead azide charges were detonated at two depths of burial, half-buried and surface-tangent below (1 DOB). The weights shown are for spherical charges. When hemispherical charges were used in the quarter-space tank, the actual weight of explosive used was one-half the nominal weight of the respective spherical charges even though the charge is referenced using its spherical weight.

Use of four colors of Ottawa Flint Shot grains as tracer particles was very successful for the experiments in Flint Shot and Banding Sand. Visibility of the grains in the desert alluvium was reduced but acceptable. However, passage of the shock wave through the alluvium resulted in the engulfment of the tracer grains by extremely fine particles of alluvium. As a result, most of the tracer grains could not be distinguished from the surrounding medium during crater formation. Film of the one alluvium event with tracers was not analyzed for particle motion data.

Use of the 1.70 g lead azide and 0.40 g PETN charges did not produce any apparent adverse effects on "normal" crater formation. Evidence of outward motion of the top edge of the Plexiglas wall (after the crater was formed) was observed in the films of the first experiments which used the 1.26 g PETN charges. In later experiments using this charge, a large steel bar was used to stiffen the top edge of the Plexiglas wall. Other than the situation just cited, no evidence of detrimental effects which could be related to use of the quarter-space tank was observed during the experimental series.

EXPERIMENTAL RESULTS

A summary of crater dimensions is presented in Table 1. In this table, dimensions of craters produced in the quarter-space tank are compared with dimensions of craters produced in normal half-space tanks. Two sets of crater dimensions are provided for the quarter-space craters. One set of values was determined from crater profile measurements made along 5 equally spaced radials. The second set of values was obtained from a profile measurement taken from the high-speed film of the experiment. In general, crater dimensions taken from the films tend to be larger than those obtained from the profile measurements. One explanation for this difference would be that the experiment is still in a dynamic situation when the crater is defined to be complete and late-time, i.e., after the film has run out, phenomena may alter the crater profile slightly. These phenomena could include a slow relaxation of compressed medium and or an accumulation of material which falls back into the crater. The effect of these various other related phenomena would be complete when the profile measurements were taken.

Crater growth rate data were obtained using a series of instantaneous crater profiles taken from films of the experiments in

TABLE 1

COMPARISION OF CRATER DIMENSIONS FROM SIMILAR EVENTS IN HALF-SPACE TANK AND QUARTER-SPACE TANK

HALF-SPACE TANK				QUARTER-SPACE TANK			
Shot I.D.	Volume, cm^3	Depth, mm	Radius, mm	Shot I.D.	Volume, cm^3	Depth, mm	Radius, mm
HALF-BURIED EVENTS IN 1.80 g/cm^3 FLINT SHOT							
1.70 Lead Azide Charge							
Avg. of	425.7	22.8	101.7	N1 (Film)	424.6	31.1	92.7
	±25	±0.8	±3	Profile Data Were Not Taken			
0.40 g PETN Charge							
Avg. of	283.3	20.7	88.4	N4 (Profile)	216.5	19.9	79.6
3 Shots	±9	±0.6	±0.8	(Film)	231.8	22.6	74.6
N2	106.4	14.8	64.6	N7 (Profile)	202.4	21.5	76.9
N8	228.6	19.0	82.6	(Film)	268.3	25.7	76.8
1.26 g PETN Charge							
Previous	639.9	25.0	117.5	N9 (Profile)	547.4	24.3	112.0
Work	706.3	26.6	120.4	(Film)	586.5	27.5	112.4
N3	647.0	24.7	118.2	N12 (Profile)	620.4	28.5	116.5
				(Film)	815.1	30.9	127.9
HALF-BURIED EVENTS IN 1.74 g/cm^3 BANDING SAND							
0.40 g PETN Charge							
Previous	201.6	17.0	82.2	N14 (Profile)	150.2	18.3	74.9
Work	191.7	16.4	81.4	(Film)	143.4	21.1	69.9
SURFACE-TANGENT BELOW EVENTS IN 1.80 g/cm^3 FLINT SHOT							
1.70 g/cm^3 Lead Azide Charge							
Avg. of	609.4	30.9	112.5	N18 (Profile)	563.8	31.0	107.1
8 Shots	±30	±1.5	±3	(Film)	668.2	35.4	102.1
0.40 g PETN Charge							
Avg. of	452.1	29.4	101.0	N10 (Profile)	314.0	24.1	90.0
3 Shots	±25	±1	±3	(Film)	388.2	27.5	89.5
N5	418.8	24.2	100.7	N11 (Profile)	332.1	24.4	92.9
				(Film)	396.0	30.1	90.8

TABLE 1 (Continued)

COMPARISON OF CRATER DIMENSIONS FROM SIMILAR EVENTS
IN HALF-SPACE TANK AND QUARTER-SPACE TANK

HALF-SPACE TANK				QUARTER-SPACE TANK			
Shot I.D.	Volume, cm^3	Depth, mm	Radius, mm	Shot I.D.	Volume, cm^3	Depth, mm	Radius, mm
SURFACE-TANGENT BELOW EVENTS (Continued) 1.26 g PETN Charge							
Avg. of 3 Shots	997.9 ±100	35.9 ±0.4	132.5 ±6	N13 (Profile)	923.0	36.9	131.0
N6	999.8	30.6	137.8	(Film)	1436.5	37.9	152.4
SURFACE-TANGENT BELOW EVENTS IN 1.74 g/cm^3 BANDING SAND							
1.70 g Lead Azide Charge							
N21	344.3	26.5	93.1	N16 (Profile)	345.2	31.0	92.8
				(Film)	296.2	37.0	76.5
0.4 g PETN Charge							
N19	267.2	24.5	85.1	N15 (Profile)	222.4	26.0	79.1
				(Film)	222.9	26.8	76.0
1.26 g PETN Charge							
N20	610.8	32.0	113.7	N23 (Profile)	620.2	34.0	116.1
				(Film)	527.4	33.1	102.0
SURFACE-TANGENT BELOW EVENTS IN 1.59 g/cm^3, DESERT ALLUVIUM (4% Moisture)							
1.7 g Lead Azide Charge							
Previous Work	145.5	27.0	73.3	N23 (Profile)	101.2	25.1	62.6
				(Film)	152.0	34.8	58.9
1.26 g PETN Charge							
Previous Work	266.0	33.0	81.7	N22 (Profile)	184.2	35.0	76.5
				(Film)	261.0	42.9	71.2

the quarter-space tank. The time interval between frames chosen for analysis increased as the time after detonation increased and the level of crater activity decreased. Time after detonation and the instantaneous crater dimensions of volume, depth, and radius were divided by the appropriate final values to produce dimensionless ratios. These dimensionless crater parameters were plotted, in Figure 1, as a function of the dimensionless time ratio to describe crater growth rate. A summary of final crater dimensions and the time of formation of these craters is presented in Table 2. Time of formation of a crater was arbitrarily defined to be that time after detonation when a slight inflection was observed on the interior wall of the ejecta plume.

Films of 10 of the 11 experiments which used the dyed sand grain tracer particles were examined using a Benson and Lehner semi-automatic film reader. In this examination, the coordinates of tracer grains were recorded on computer cards for subsequent processing in a data-handling computer program. A total of 146 frames from the 10 films were examined and 15,388 pairs of readings of grain coordinates were made. Two types of information are produced and printed during processing of raw data from each frame of film. A copy of each type of data is presented in Figures 2 and 3. In these figures, data for tracer grains near the surface of the right side of the test bed are shown in the column along the left side of the page; grains in the successively lower rows of tracers appear in columns further to the right of this column. Integers just below the page heading and at the extreme left of the page are row and column subscripts used to identify the various grains.

In Figure 2, values at the intersections of the row and column integers are the X and Y coordinates of the grains in mm. The values centered inside each group of four grains are related to the properties of material inside the area, a trapezium, bounded by these grains. These properties are (1) the X and Y coordinates, in mm, of the center of gravity of the trapezium, (2) the instantaneous average density, in g/cm^3, of material within a ring whose cross section is the trapezium and (3) and indicator of the shear

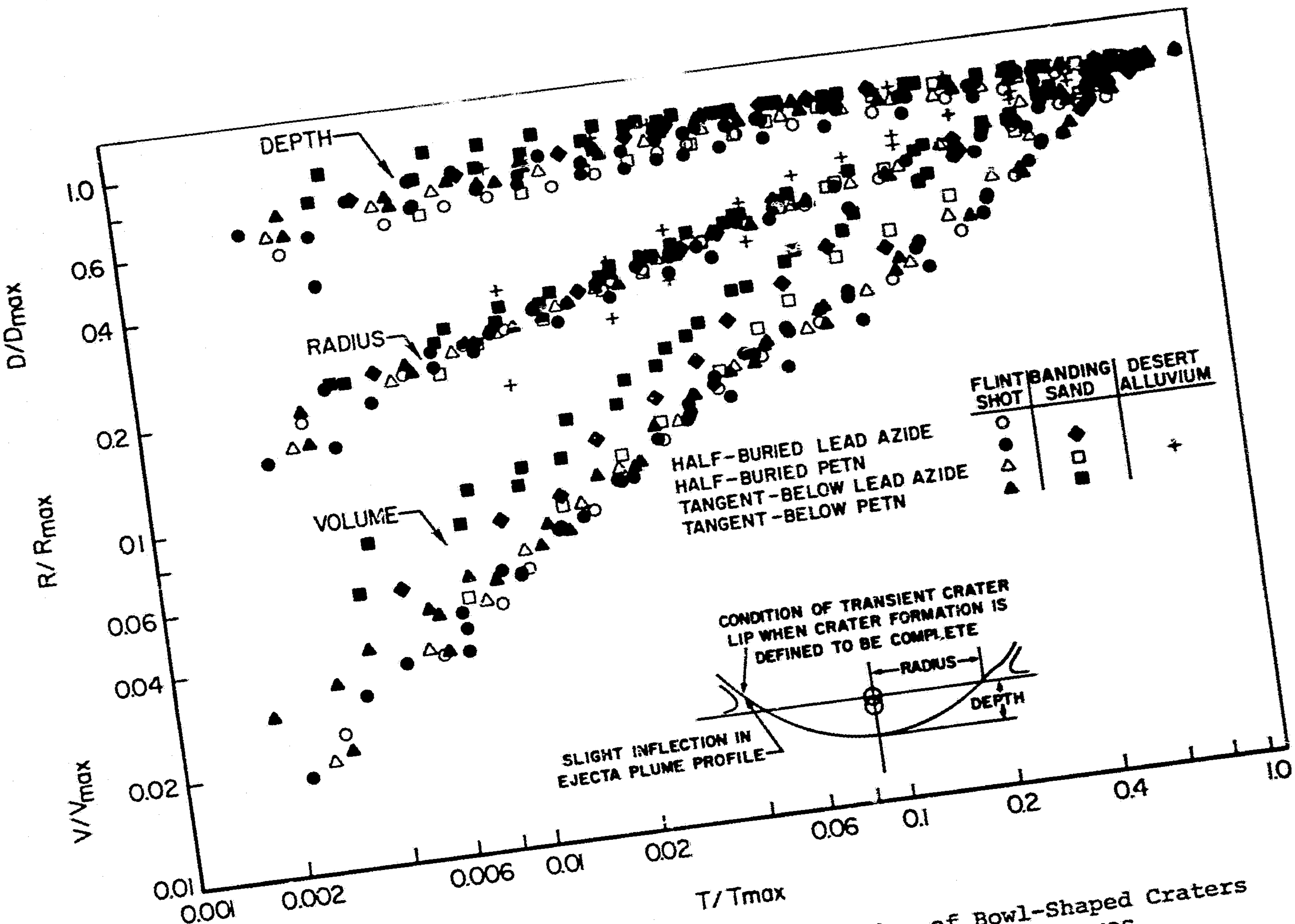

Figure 1. Rate of Growth of Volume, Depth, and Radius of Bowl-Shaped Craters Produced by the Detonation of Small High-Explosive Charges.

TABLE 2

CRATER GROWTH RATE SUMMARY

Event[a]		Explosive/ Configuration	Formation Time, msec	Volume, cm^3	Depth, mm	Radius, mm
		1.80 g/cm^3 FLINT SHOT				
N1	P	PbN_6, Half-Buried	58	425	31	93
N18	P	PbN_6, 1 DOB	63	668	35	103
N4		0.40 PETN, Half-Buried	47	232	22	75
N7	P	0.40 PETN, Half-Buried	47	268	26	77
N10	P	0.40 PETN, 1 DOB	59	388	28	90
N11	P	0.40 PETN, 1 DOB	58	394	30	91
N9[b]		1.26 PETN, Half-Buried	71	587	27	112
N12[b,c]	P	1.26 PETN, Half-Buried	72	815	31	128
N13[b,c]	P	1.26 PETN, 1 DOB	92	1437	38	152
		1.74 g/cm^3 BANDING SAND				
N16	P	PbN_6, 1 DOB	23	296	37	76
N14	P	0.40 PETN, Half-Buried	35	143	21	70
N15	P	0.40 PETN, 1 DOB	46	223	27	76
N17[d]	P	1.26 PETN, 1 DOB	43	527	33	102
		1.59 g/cm^3 DESERT ALLUVIUM (4% Moisture)				
N23		PbN_6, 1 DOB	14	152	35	59
N22[b,d]	P[e]	1.26 PETN, 1 DOB	12	291	45	66

[a] P after event name indicates tracer particles were used

[b] Crater-medium interface poorly defined

[c] Evidence of forward motion of Plexiglas wall about 8 msec after detonation

[d] Bar stiffener used

[e] Tracer particles engulfed by fine material in alluvium

SHOT NUMBER -- HPPETN-256-N13 (0.2251 GM PETN CHARGE)
SURFACE-TANGENT BELOW IN COARSE OTTAWA SAND

FRAME NUMBER -- 5 (0.785 MSEC AFTER DETONATION)

PARTICLE LOCATION AND MATERIAL PROPERTY DATA

		1	2	3	4	5	6	7	8	9
1	X	******	******	******	1.08	0.66	-0.03	0.77	0.32	1.66
	Y	******	******	******	-27.65	-34.66	-42.67	-50.21	-57.91	-65.19
	X-CG	******	******	******	5.28	4.67	4.89	4.62	5.13	
	Y-CG	******	******	******	-31.60	-38.73	-46.35	-53.90	-61.30	
	DENS	*****	*****	*****	1.525	1.739	1.803	1.799	1.667	
	SS	******	******	******	0.0606	0.0444	0.0200	0.0229	-0.0191	
2	X	******	******	11.31	9.95	9.15	9.03	8.33	8.68	9.40
	Y	******	******	-19.91	-26.98	-34.82	-42.62	-50.20	-57.91	-65.93
	X-CG	******	******	14.91	13.80	13.32	13.03	12.96	12.99	
	Y-CG	******	******	-23.02	-30.60	-38.38	-46.31	-53.89	-61.72	
	DENS	*****	*****	1.478	1.603	1.729	1.696	1.782	1.789	
	SS	******	******	0.2930	0.1332	0.0612	0.0089	-0.0433	0.0512	
3	X	******	23.19	19.67	18.61	17.73	17.38	17.31	17.16	17.17
	Y	******	-8.83	-19.33	-26.79	-34.50	-42.37	-49.96	-57.08	-65.77
	X-CG	******	24.76	22.88	22.07	21.66	21.38	21.27	21.12	
	Y-CG	******	-13.34	-23.13	-30.29	-38.29	-45.87	-53.73	-61.69	
	DENS	*****	1.522	1.667	1.682	1.749	1.837	1.904	1.833	
	SS	******	0.3460	0.2663	0.1796	0.1112	1.1399	0.0396	0.0608	
4	X	32.94	29.37	27.08	26.46	25.54	25.02	25.22	25.32	25.98
	Y	7.47	-8.36	-17.36	-25.88	-34.01	-41.99	-49.30	-57.76	-65.49
	X-CG	33.26	31.69	30.66	30.04	29.93	29.76	29.33	29.33	
	Y-CG	-1.80	-12.86	-21.32	-29.94	-37.79	-45.37	-53.39	-61.31	
	DENS	1.576	1.644	1.649	1.711	1.734	1.703	1.730	1.729	
	SS	-0.3243	0.1002	0.1273	0.0696	0.0730	0.0709	0.0080	-0.0058	
5	X	36.08	35.40	34.81	34.14	34.19	34.22	33.63	33.29	33.77
	Y	2.76	-7.90	-16.90	-25.94	-33.61	-41.65	-49.30	-57.32	-65.18
	X-CG	39.00	38.76	38.25	37.95	37.83	37.69	37.36	37.59	
	Y-CG	-5.09	-12.39	-21.46	-29.38	-37.31	-45.65	-53.33	-61.20	
	DENS	1.672	1.679	1.725	1.662	1.780	1.769	1.769	1.741	
	SS	-0.0626	0.0752	0.0929	0.0799	0.0295	0.0643	0.0133	[illegible]	
6	X	42.29	42.83	41.99	42.14	41.36	41.38	41.20	41.20	41.91
	Y	1.28	-7.95	-16.96	-25.74	-33.33	-41.37	-49.30	-57.23	-65.07
	X-CG	46.07	46.10	45.90	45.75	45.56	45.60	45.31	45.93	
	Y-CG	-3.39	-12.35	-21.13	-29.66	-37.19	-45.32	-53.30	-61.26	
	DENS	1.737	1.723	1.707	1.737	1.767	1.811	1.785	1.766	
	SS	-0.0721	0.0179	0.0763	0.0835	0.0566	0.0272	0.0231	0.0366	
7	X	49.30	49.94	49.82	49.71	49.71	49.39	49.44	49.18	49.98
	Y	0.67	-6.32	-16.71	-25.30	-33.15	-41.04	-49.40	-57.33	-65.36
	X-CG	53.44	53.73	53.63	53.51	53.65	53.48	53.19	53.30	
	Y-CG	-3.97	-12.37	-21.05	-29.28	-37.10	-45.26	-53.27	-61.19	
	DENS	1.703	1.730	1.791	1.817	1.756	1.743	1.833	1.805	
	SS	-0.0628	-0.0236	0.0429	0.0755	0.0523	0.0140	0.0326	-0.0035	
8	X	56.87	57.65	57.59	57.29	57.45	57.09	57.12	57.16	57.29
	Y	0.41	-8.57	-16.67	-25.39	-33.02	-41.08	-49.98	-57.08	-65.06
	X-CG	61.22	61.42	61.37	61.82	61.55	61.33	61.26	61.26	
	Y-CG	-4.24	-12.77	-21.13	-29.17	-37.17	-45.38	-53.29	-61.07	
	DENS	1.772	1.841	1.767	1.799	1.781	1.800	1.819	1.800	
	SS	-0.0431	-0.0476	0.0221	0.2042	-0.0085	0.0161	0.0288	0.0083	
9	X	65.12	65.33	65.32	65.32	65.49	65.36	65.30	65.30	65.17
	Y	-0.39	-8.52	-17.27	-24.89	-33.27	-41.37	-49.41	-57.09	-65.12
	X-CG	69.25	69.21	69.31	69.35	69.38	69.23	69.33	69.25	
	Y-CG	-4.40	-12.87	-21.00	-29.17	-37.13	-45.27	-53.03	-60.94	
	DENS	1.798	1.857	1.809	1.817	1.820	1.800	1.787	1.846	
	SS	-0.0055	0.0130	-0.0060	0.0200	0.0017	0.0263	0.0137	0.0107	
10	X	73.37	72.88	73.12	72.92	73.54	72.79	73.36	73.33	73.05
	Y	-0.25	-8.75	-16.86	-25.06	[illegible]	-41.04	-48.96	-56.67	-64.94
	X-CG	76.99	77.01	77.05	77.15	76.94	77.04	77.44	77.07	
	Y-CG	-4.60	-12.81	-20.90	-28.98	-37.12	-44.98	-53.00	-60.94	
	DENS	1.848	1.799	1.798	1.758	1.816	1.786	1.785	1.841	
	SS	-0.0169	-0.0080	-0.0414	0.0400	0.0068	-0.0065	0.0353	0.0147	
11	X	80.74	80.95	81.13	81.14	80.95	80.57	81.49	81.31	80.91
	Y	-0.28	-8.84	-16.84	-24.77	-33.14	-40.92	-48.94	-57.47	-64.70
	X-CG	84.66	84.80	85.14	85.14	84.97	85.02	85.02	85.00	
	Y-CG	-4.74	-12.91	-20.80	-28.89	-37.04	-44.93	-53.17	-61.16	
	DENS	1.754	1.773	1.805	1.797	1.845	1.837	1.832	1.800	
	SS	0.0062	-0.0068	-0.0259	-0.0127	0.0209	-0.0077	-0.0120	0.0281	
12	X	88.35	88.08	89.00	89.31	89.19	89.07	88.92	88.51	89.11
	Y	-1.21	-6.83	-16.86	-24.66	-32.98	-41.02	-49.21	-57.16	-64.90
	X-CG	92.79	92.73	93.01	93.16	93.07	92.77	92.92	92.99	
	Y-CG	-4.89	-12.79	-20.79	-28.87	-37.03	-44.79	-52.92	-60.96	
	DENS	1.723	1.827	1.821	1.838	1.812	1.738	1.798	1.833	
	SS	0.0252	-0.0037	-0.0171	0.0006	-0.0016	0.0041	0.0065	0.0233	
13	X	96.83	97.36	96.59	97.11	[illegible]	96.99	96.38	97.26	97.06
	Y	-0.11	-9.19	-16.86	-24.75	-33.09	-41.09	-47.89	-57.08	-64.95
	X-CG	100.86	100.86	100.86	100.80	100.87	100.97	100.75	101.21	
	Y-CG	-4.67	-13.01	-20.92	-28.96	-36.94	-44.71	-52.46	-60.90	
	DENS	1.758	1.839	1.758	1.791	1.827	1.840	1.786	1.794	
	SS	0.0531	0.0421	-0.0226	0.0365	-0.0219	0.0022	0.0258	0.0286	
14	X	105.00	104.57	104.79	104.86	104.55	104.88	104.93	104.87	105.31
	Y	-0.92	-8.83	-16.86	-25.40	-32.69	-40.76	-48.92	-56.20	-65.15
	X-CG	108.82	108.81	108.82	108.85	108.76	108.82	108.95	108.96	
	Y-CG	-4.92	-12.81	-21.05	-29.05	-36.63	-44.81	-52.70	-60.65	
	DENS	1.792	1.730	1.792	1.826	1.835	1.857	1.842	1.772	
	SS	0.0351	-0.0074	-0.0264	0.0380	0.0106	-0.0209	0.0001	0.0128	
15	X	112.79	112.93	112.93	112.81	112.09	112.61	112.80	113.05	112.73
	Y	-0.95	-8.79	-16.84	-25.16	-32.75	-40.58	-48.93	-56.64	-64.91
	X-CG	116.93	116.85	116.73	116.85	116.74	116.66	116.77	116.65	
	Y-CG	-4.96	-12.69	-21.01	-28.79	-36.68	-44.66	-52.77	-61.04	
	DENS	1.821	1.816	1.806	1.809	1.825	1.773	1.850	1.791	
	SS	-0.0426	-0.0141	-0.0016	0.0138	0.0190	-0.0104	0.0025	-0.0234	
16	X	121.20	120.89	123.60	120.81	120.60	120.64	120.70	120.24	120.69
	Y	-1.34	-8.39	[illegible]	-24.75	-32.43	-40.58	-48.57	-57.17	-65.18

Figure 2. Particle Location and Material Property Data Printout.

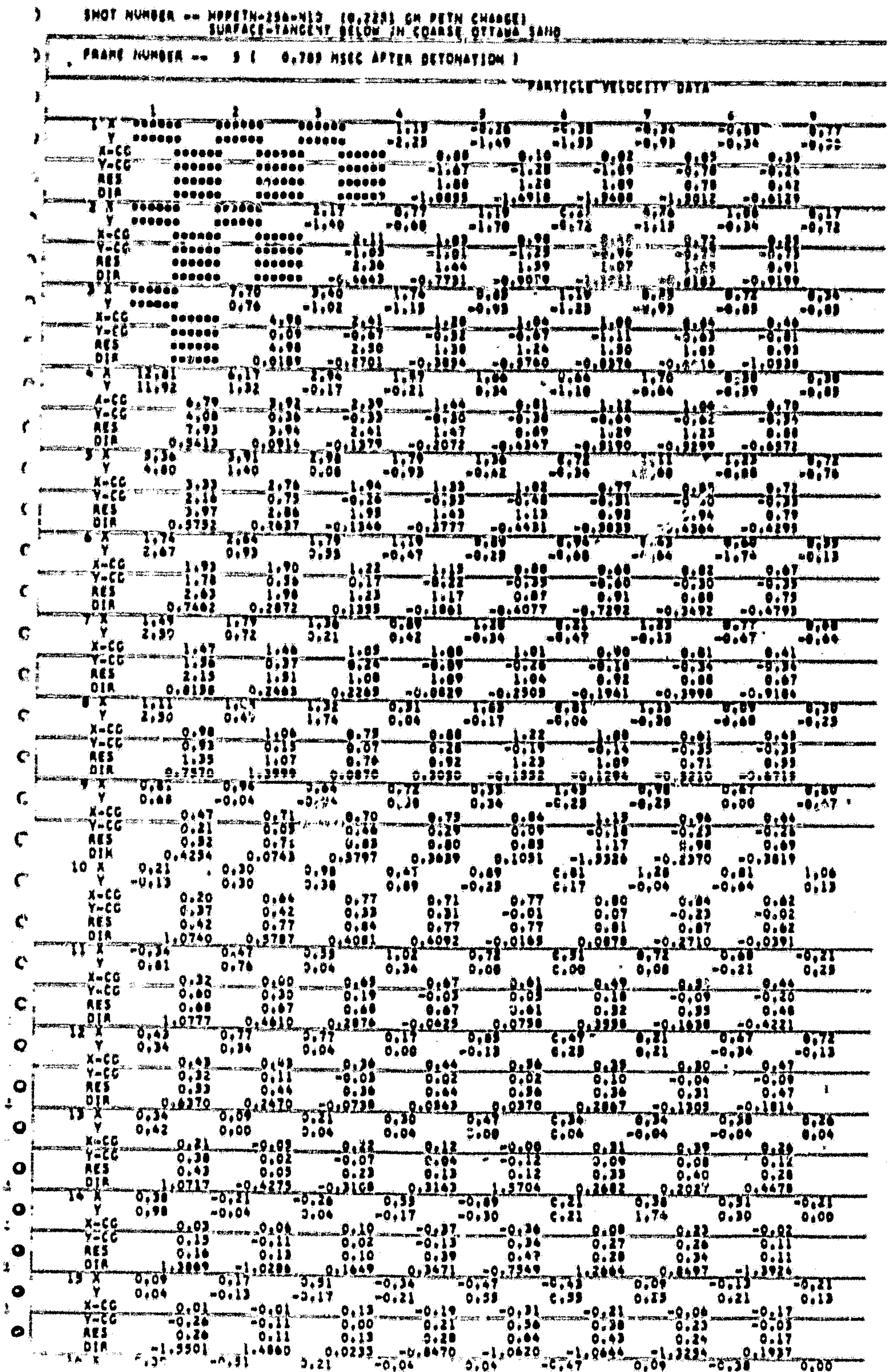

Figure 3. Particle Velocity Data Printout

deformation, in radians, exhibited within the region enclosed by the quadrilateral.

In Figure 3, the X and Y component of individual grain velocities are given in m/sec at the intersection of the row and column integers. The velocity components and resultant velocity of the center of gravity of each of the regions, in m/sec, is given at the center of each area. The direction of the resultant velocity vector, in radians, is also included in this zonal information.

The originals of the computer printouts shown in Figures 2 and 3 have been loosely bound in 10 separate volumes (1 per shot) to protect and preserve them for later use. The manner in which they have been bound facilitates reproduction for distribution of the information to interested parties.

DISCUSSION

Study of particle motions observed for the experiments in the quarter-space tank indicate that the behavior of material in the region below and around the crater is essentially the same, regardless of the cratering medium. Further, an effective center of disturbance, i.e., apparent origin of particle trajectories, is concentrated in a very small region along the crater axis at the base of the explosive charge. A consistent pattern of "failure" of uncratered medium was also observed in each of the experiments. Using the "SS" values shown in Figure 2 to place limits on the extent of shear deformation experienced by each quadrilateral zone, four relatively distinct regions were identified. Beginning at the axis and floor of the crater, these regions are: (1) 0° to 30° (angles are measured with respect to axis of crater and are approximate values) - axial compression of material; (2) 30° to 60° - significant shear deformation, values in excess of 0.44 radians were common: (3) 60° to 80° - radial compression and small amounts of shear deformation; and (4) 80° to 90° - negative shear deformation, i.e., outward motion of subsurface material exceeded motion of surface material. As mentioned, these modes of deformation were consistently observed in data obtained from analysis of all 10 particle displacement experiments.

The crater growth rate data showed that the rate of growth of a crater was strongly dependent on the characteristics of the cratering medium and only very weakly dependent on the composition, size, and depth of burial of the explosive charge. Data presented in Table 2 would suggest that crater formation times and dimensions may be related to some characteristic parameter(s) of the cratering medium, e.g., the average dimension of a grain or particle of the cratered material. Crater formation times and crater dimensions decreased significantly as the average grain size of the cratered medium decreased.

Craters formed in Banding Sand and the desert alluvium exhibited several late-time features near the flanks of the crater that were not exhibited in craters formed in Flint Shot. In Banding Sand, low-velocity fallback from the ejecta plum was deposited on the upper regions of the crater walls. In the desert alluvium, a normal bowl-shaped crater was formed; however, the bowl shape was subsequently altered when a characteristic bench evolved as material in the flanks of the crater continued to be carried away.

Flint Shot was a very well behaved material and proved ideal for use as a benchmark or base line cratering medium. The Banding Sand also proved relatively easy to work with. The desert alluvium was more difficult since care had to be taken prior to and during use of this material to maintain its moisture content and in-situ density. The larger PETN charges used in the study probably exceeded the size which can be reliably used for experiments of this type. The smaller charges were very well behaved.

PUBLICATIONS

Three publications, all entitled "Formation of Bowl-Shaped Craters" were prepared to present and discuss various aspects of the work funded by NSG-7444. An abstract of a paper was published in Lunar and Planetary Science XI, pages 877-878. At the invitation and request of the Conference Program Committee, and extended lay-language version of this abstract was prepared and submitted to the Lunar and Planetary Institute for inclusion in a press package that was distributed before and during the 11th Lunar and Planetary Science Conference. Finally, a paper presented at the 11th Lunar and Planetary Science Conference was published in the proceedings of that conference on pages 2129-2144.

Alan Landsburg Productions, Los Angeles, California, producers of the television program "In Search Of", contacted the University and requested to review copies of various cratering films for possible inclusion in one of their programs. Films of experiments in the quarter-space tank were included in a preliminary edition of a program but were deleted when the program length had to be shortened.